On the Directionality of Cation/Molecule Bonding in Lewis Bases Containing the Carbonyl Group

Younes Valadbeigi[†] and Jean-François Gal[‡]

[†]Department of Chemistry, Science and Research Branch, Islamic Azad University, Tehran, Iran

[‡]Institut de Chimie de Nice, UMR 7272, Université Côte d'Azur, CNRS, 06108 Nice, France

Supplementary Material

Content page

Table S1. Calculated gas phase cation affinities (CA) and cation basicities (CB) of the studied molecules by B3LYP/6-311++G(d,p) method at 298.15K. Im: Imidazolone; Lactone: gamma-butyrolactone; Cyt: Cytosine. Isomers a, b, and c correspond to cation attachment from different sites, see main text, Figs. 4 & 6. Experimental values given in parenthesis for comparison; values in **bold** correspond to experiments involving different tautomers, see text and Fig. S8.

	CA ($-\Delta H$)/kJ.mol^{-1}	CB ($-\Delta G$)/kJ.mol^{-1}
$CH_2O + H^+ \rightarrow [CH_2O\text{-}H]^+$	705.5 (712.9)[b]	673.1 (683.3)[b]
$CH_3CHO + H^+ \rightarrow [CH_3CHO\text{-}H]^+$	771.1 (768.5)[b]	739.2 (736.5)[b]
$(CH_3)_2CO + H^+ \rightarrow [(CH_3)_2CO\text{-}H]^+$	814.1 (812)[b]	781.8
$Im + H^+ \rightarrow [Im\text{-}H]^+$ (N)[a]	818.3	787.1
$Im + H^+ \rightarrow [Im\text{-}H]^+$ (O)	739.4	707.8
$Lactone + H^+ \rightarrow [Lactone\text{-}H]^+$	841.7 (840.0)[b]	809.3 (808.1)[b]
$Cyt + H^+ \rightarrow [Cyt\text{-}H]^+$ (N)	956.0 (949.9)[b]	922.2 (918.0)[b]
$Cyt + H^+ \rightarrow [Cyt\text{-}H]^+$ (O)	954.7	919.9
$CH_2S + H^+ \rightarrow [CH_2S\text{-}H]^+$	764.3 (759.7)[b]	733.3 (730.5)[b]
$CH_2Se + H^+ \rightarrow [CH_2Se\text{-}H]^+$	774.5 (764.0)[b]	743.7 (734.9)[b]
$CH_2O + Li^+ \rightarrow [CH_2O\text{-}Li]^+$	145.6 (142)[c]	116.5 (116.6)[d]
$CH_3CHO + Li^+ \rightarrow [CH_3CHO\text{-}Li]^+$	173.3 (170)[c]	143.6 (144.1)[d]
$(CH_3)_2CO + Li^+ \rightarrow [(CH_3)_2CO\text{-}Li]^+$	192.6 (186)[e]	163.1 (156.7)[d]
$Im + Li^+ \rightarrow [Im\text{-}Li]^+$-a	167.9	140.1
$Im + Li^+ \rightarrow [Im\text{-}Li]^+$-b	175.9	143.5
$Lactone + Li^+ \rightarrow [Lactone\text{-}Li]^+$	219.7	192.8
$Cyt + Li^+ \rightarrow [Cyt\text{-}Li]^+$-a	289.3 (**235, 237**)[c]; (285.1)[f]	253.8
$Cyt + Li^+ \rightarrow [Cyt\text{-}Li]^+$-b	278.2	247.7
$CH_2S + Li^+ \rightarrow [CH_2S\text{-}Li]^+$	111.5	82.9
$CH_2Se + Li^+ \rightarrow [CH_2Se\text{-}Li]^+$	114.1	85.6
$CH_2O + Na^+ \rightarrow [CH_2O\text{-}Na]^+$	102.6 (96)[e]	74.9
$CH_3CHO + Na^+ \rightarrow [CH_3CHO\text{-}Na]^+$	123.1 (119)[d]; (113)[c]	95.0 (92)[d]
$(CH_3)_2CO + Na^+ \rightarrow [(CH_3)_2CO\text{-}Na]^+$	137.4 (131.3)[d]	109.3 (105.7)[d]
$Im + Na^+ \rightarrow [Im\text{-}Na]^+$-a	120.9	94.5
$Im + Na^+ \rightarrow [Im\text{-}Na]^+$-b	128.5	97.6
$Lactone + Na^+ \rightarrow [Lactone\text{-}Na]^+$	160.3	135.0
$Cyt + Na^+ \rightarrow [Cyt\text{-}Na]^+$	217.7 (**176**, **178**, 210)[c]; (215.1)[f]	183.8
$CH_2S + Na^+ \rightarrow [CH_2S\text{-}Na]^+$	75.6	48.5
$CH_2Se + Na^+ \rightarrow [CH_2Se\text{-}Na]^+$	78.6	51.6
$CH_2O + K^+ \rightarrow [CH_2O\text{-}K]^+$	78.4	52.2
$CH_3CHO + K^+ \rightarrow [CH_3CHO\text{-}K]^+$	94.2	67.4
$(CH_3)_2CO + K^+ \rightarrow [(CH_3)_2CO\text{-}K]^+$	102.8 (102.1)[d]	80.1
$Im + K^+ \rightarrow [Im\text{-}K]^+$-a	90.1	65.3
$Im + K^+ \rightarrow [Im\text{-}K]^+$-b	92.8	64.2
$Lactone + K^+ \rightarrow [Lactone\text{-}K]^+$	122.4	98.3
$Cyt + K^+ \rightarrow [Cyt\text{-}K]^+$	165.8 (**110, 136,** 162)[c]; (161.4)[f]	134.8
$CH_2S + K^+ \rightarrow [CH_2S\text{-}K]^+$	45.5	20.9
$CH_2Se + K^+ \rightarrow [CH_2Se\text{-}K]^+$	46.5	22.0
$CH_2O + Al^+ \rightarrow [CH_2O\text{-}Al]^+$	114.8 (115.1)[d,e]	88.8 (93.6)[d]; (90.3)[e]
$CH_3CHO + Al^+ \rightarrow [CH_3CHO\text{-}Al]^+$	150.5 (156.8)[e]	122.9 (130.0)[d]; (129.8)[e]
$(CH_3)_2CO + Al^+ \rightarrow [(CH_3)_2CO\text{-}Al]^+$	175.5	151.8 (157.6)[d]
$Im + Al^+ \rightarrow [Im\text{-}Al]^+$-a	134.3	101.9
$Im + Al^+ \rightarrow [Im\text{-}Al]^+$-b	132.2	106.2
$Im + Al^+ \rightarrow [Im\text{-}Al]^+$-c	126.5	98.9
$Lactone + Al^+ \rightarrow [Lactone\text{-}Al]^+$	202.6	176.8
$Cyt + Al^+ \rightarrow [Cyt\text{-}Al]^+$	286.4	253.9
$CH_2S + Al^+ \rightarrow [CH_2S\text{-}Al]^+$	89.8	62.7
$CH_2Se + Al^+ \rightarrow [CH_2Se\text{-}Al]^+$	97.9	70.8
$CH_2O + Cu^+ \rightarrow [CH_2O\text{-}Cu]^+$	177.1 (165)[e]	146.3
$CH_3CHO + Cu^+ \rightarrow [CH_3CHO\text{-}Cu]^+$	209.3	177.9
$(CH_3)_2CO + Cu^+ \rightarrow [(CH_3)_2CO\text{-}Cu]^+$	222.7	196.5
$Im + Cu^+ \rightarrow [Im\text{-}Cu]^+$-a	266.4	232.6
$Lactone + Cu^+ \rightarrow [Lactone\text{-}Cu]^+$	264.5	234.2
$Cyt + Cu^+ \rightarrow [Cyt\text{-}Cu]^+$-a	361.6	319.3
$CH_2S + Cu^+ \rightarrow [CH_2S\text{-}Cu]^+$	221.8	190.4
$CH_2Se + Cu^+ \rightarrow [CH_2Se\text{-}Cu]^+$	235.1	203.9

[a] The atoms in parenthesis are the sites of protonation.
[b] From ref. [10] (298 K).
[c] Re-anchored CA values at 0 K for alkali cations/cytosine compiled in ref. [2] (values at 298 K are 1-3 kJ/mol larger).
[d] From ref. [5] (298 K). [e] From ref. [13] (298K). [f] Calculated by B3LYP/def2-TZVPPD method, ref. [45].

Table S2. The ionization energies of the metals studied in this work. The calculations were performed at the B3LYP/6-311++G(d,p) level of theory.

Atom	B3LYP/6-311++G(d,p)	Experimental[a]
H	13.66	13.59
Li	5.61	5.39
Na	5.42	5.14
K	4.49	4.34
Al	6.01	5.99
Cu	8.03	7.73

[a] from www.webbook.nist.gov

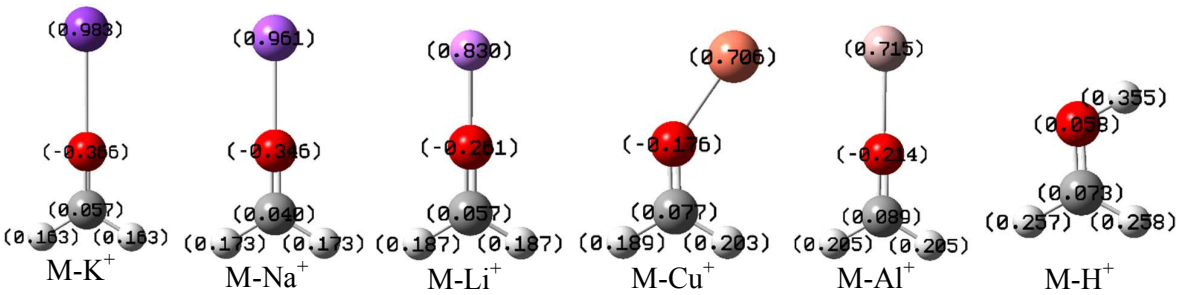

Figure S1. Mulliken charge distribution computed by B3LYP/6-311++G(d,p). Cation with smaller charge indicates more covalent interaction.

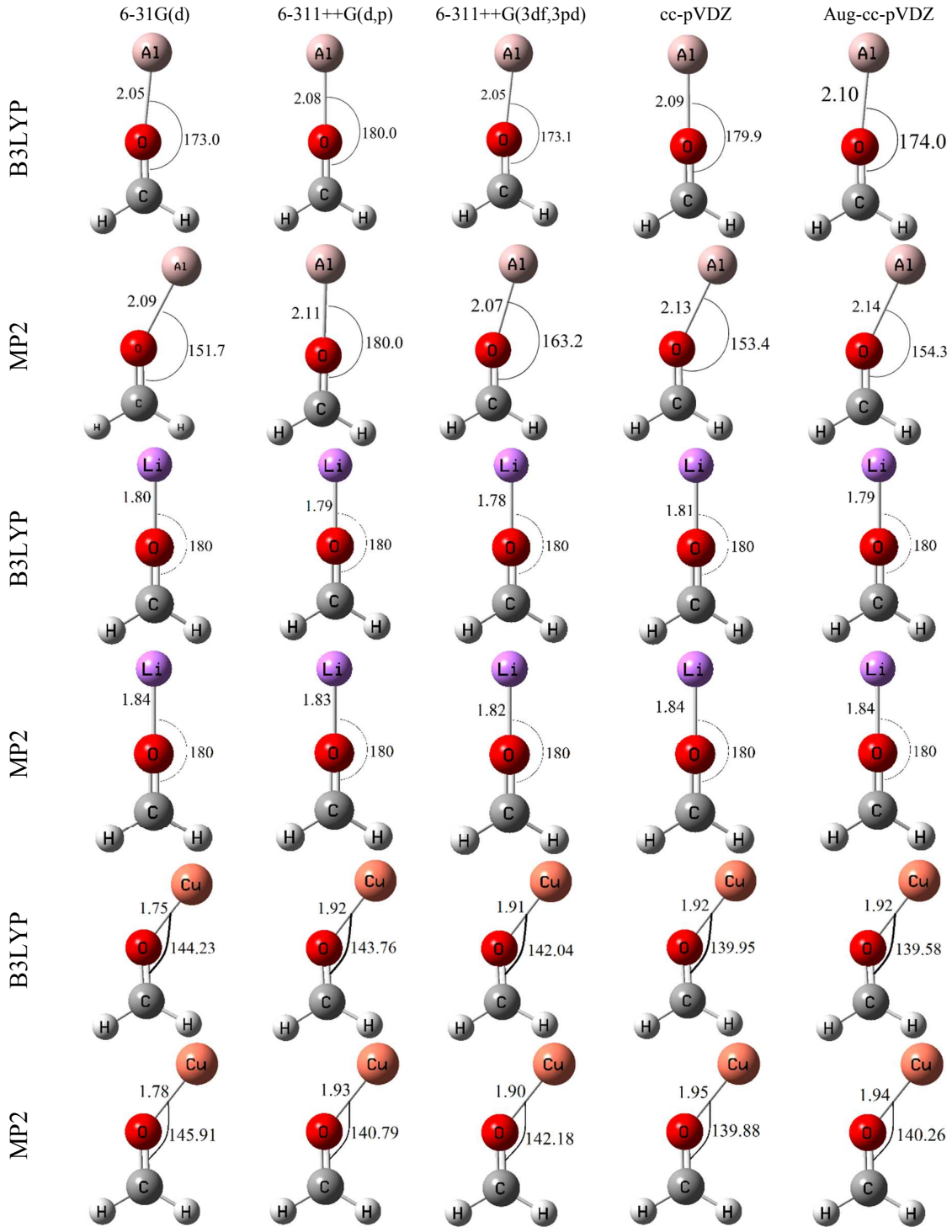

Figure S2. Effect of computational methods and basis sets on the C=O-X angle in the CH_2O/X^+ adduct ions (X=Al, Li, Cu).

Table S3. The calculated ρ, $\nabla^2\rho$, $G(r)$ and $V(r)$ at the bond critical point (BCP) of the cation/molecule interactions. The atom in parenthesis indicates the site of interaction with the cation.

Adduct ion	$\rho(r)$	$\nabla^2\rho(r)$	$G(r)$	$V(r)$	H(r)	$-G(r)/V(r)$
$[CH_2O\text{-}H]^+$	0.339	-2.515	0.0472	-0.7233	-0.6760	0.065
$[CH_2O\text{-}Cu]^+$	0.086	0.533	0.1394	-0.1454	-0.0060	0.958
$[CH_2O\text{-}Al]^+$	0.039	0.152	0.0410	-0.0438	-0.0028	0.935
$[CH_2O\text{-}Li]^+$	0.037	0.320	0.0648	-0.0494	0.0153	1.311
$[CH_2O\text{-}Na]^+$	0.026	0.195	0.0396	-0.0303	0.0092	1.306
$[CH_2O\text{-}K]^+$	0.021	0.115	0.0237	-0.0187	0.0050	1.266
$[CH_3CHO\text{-}H]^+$	0.345	-2.540	0.0512	-0.7376	-0.6863	0.069
$[CH_3CHO\text{-}Cu]^+$	0.090	0.554	0.1459	-0.1532	-0.0073	0.952
$[CH_3CHO\text{-}Al]^+$	0.046	0.236	0.0593	-0.0596	-0.0003	0.995
$[CH_3CHO\text{-}Li]^+$	0.040	0.352	0.0718	-0.0555	0.0162	1.293
$[CH_3CHO\text{-}Na]^+$	0.028	0.215	0.0438	-0.0339	0.0099	1.293
$[CH_3CHO\text{-}K]^+$	0.023	0.128	0.0268	-0.0215	0.0053	1.248
$[Im\text{-}H]^+$ (O)	0.338	-2.502	0.0489	-0.7237	-0.6747	0.067
$[Im\text{-}H]^+$ (N)	0.327	-1.797	0.0372	-0.5238	-0.4865	0.071
$[Im\text{-}Cu]^+$-a (N)	0.102	0.473	0.1400	-0.1618	-0.0217	0.866
$[Im\text{-}Al]^+$-a (O)	0.043	0.193	0.0499	-0.0514	-0.0014	0.971
$[Im\text{-}Al]^+$-b (O)	0.043	0.168	0.0457	-0.0494	-0.0036	0.926
$[Im\text{-}Al]^+$-c (N)	0.038	0.069	0.0258	-0.0342	-0.0084	0.754
$[Im\text{-}Li]^+$-a (O)	0.038	0.333	0.0675	-0.0517	0.0158	1.305
$[Im\text{-}Li]^+$-b (O)	0.024	0.154	0.0321	-0.0256	0.0064	1.251
$[Im\text{-}Li]^+$-b (N)	0.023	0.142	0.0295	-0.0234	0.0061	1.262
$[Im\text{-}Na]^+$-a (O)	0.027	0.203	0.0412	-0.0316	0.0096	1.303
$[Im\text{-}Na]^+$-b (O)	0.018	0.101	0.0212	-0.0171	0.0041	1.236
$[Im\text{-}Na]^+$-b (N)	0.017	0.096	0.0197	-0.0155	0.0043	1.275
$[Im\text{-}K]^+$-a (O)	0.022	0.119	0.0247	-0.0195	0.0052	1.265
$[Im\text{-}K]^+$-b (O)	0.016	0.047	0.0150	-0.0125	0.0025	1.201
$[Im\text{-}K]^+$-b (N)	0.013	0.053	0.0108	-0.0085	0.0023	1.274
$[Lactone\text{-}H]^+$	0.345	-2.510	0.0544	-0.7365	-0.6822	0.074
$[Lactone\text{-}Cu]^+$	0.093	0.586	0.1551	-0.1634	-0.0083	0.949
$[Lactone\text{-}Al]^+$	0.053	0.326	0.0796	-0.0775	0.0021	1.027
$[Lactone\text{-}Li]^+$	0.044	0.381	0.0786	-0.0618	0.0168	1.271
$[Lactone\text{-}Na^+$	0.031	0.229	0.0472	-0.0370	0.0102	1.275
$[Lactone\text{-}K]^+$	0.026	0.140	0.0295	-0.0241	0.0054	1.224
$[Cyt\text{-}Cu]^+$-a (O)	0.054	0.256	0.0669	-0.0697	-0.0028	0.959
$[Cyt\text{-}Cu]^+$-a (N)	0.069	0.318	0.0885	-0.0972	-0.0087	0.909
$[Cyt\text{-}Al]^+$ (O)	0.064	0.446	0.1075	-0.1034	0.0041	1.039
$[Cyt\text{-}Li]^+$-a (O)	0.037	0.264	0.0554	-0.0449	0.0105	1.234
$[Cyt\text{-}Li]^+$-a (N)	0.022	0.141	0.0296	-0.0240	0.0056	1.235
$[Cyt\text{-}Li]^+$-b (O)	0.048	0.403	0.0849	-0.0688	0.0161	1.233
$[Cyt\text{-}Na]^+$ (O)	0.028	0.179	0.0378	-0.0307	0.0071	1.231
$[Cyt\text{-}Na]^+$ (N)	0.016	0.091	0.0188	-0.0150	0.0038	1.255
$[Cyt\text{-}K]^+$ (O)	0.027	0.124	0.0274	-0.0236	0.0037	1.159
$[Cyt\text{-}K]^+$ (N)	0.012	0.048	0.0099	-0.0079	0.0020	1.257
$[CH_2S\text{-}H]^+$	0.219	-0.664	0.0308	-0.2277	-0.1969	0.135
$[CH_2S\text{-}Cu]^+$	0.083	0.197	0.0743	-0.0992	-0.0249	0.748
$[CH_2S\text{-}Al]^+$	0.034	-0.009	0.0084	-0.0191	-0.0107	0.441
$[CH_2S\text{-}Li]^+$	0.025	0.095	0.0232	-0.0225	0.0007	1.031
$[CH_2S\text{-}Na]^+$	0.018	0.070	0.0157	-0.0139	0.0018	1.126
$[CH_2S\text{-}K]^+$	0.012	0.039	0.0083	-0.0069	0.0014	1.204
$[CH_2Se\text{-}H]^+$	0.176	-0.322	0.0549	-0.1905	-0.1356	0.288
$[CH_2Se\text{-}Cu]^+$	0.075	0.155	0.0610	-0.0732	-0.0122	0.833
$[CH_2Se\text{-}Al]^+$	0.033	-0.011	0.0071	-0.0169	-0.0098	0.417
$[CH_2Se\text{-}Li]^+$	0.023	0.081	0.0198	-0.0192	0.0006	1.029
$[CH_2Se\text{-}Na]^+$	0.016	0.061	0.0136	-0.0153	-0.0016	0.894
$[CH_2Se\text{-}K]^+$	0.012	0.034	0.0072	-0.0060	0.0012	1.201

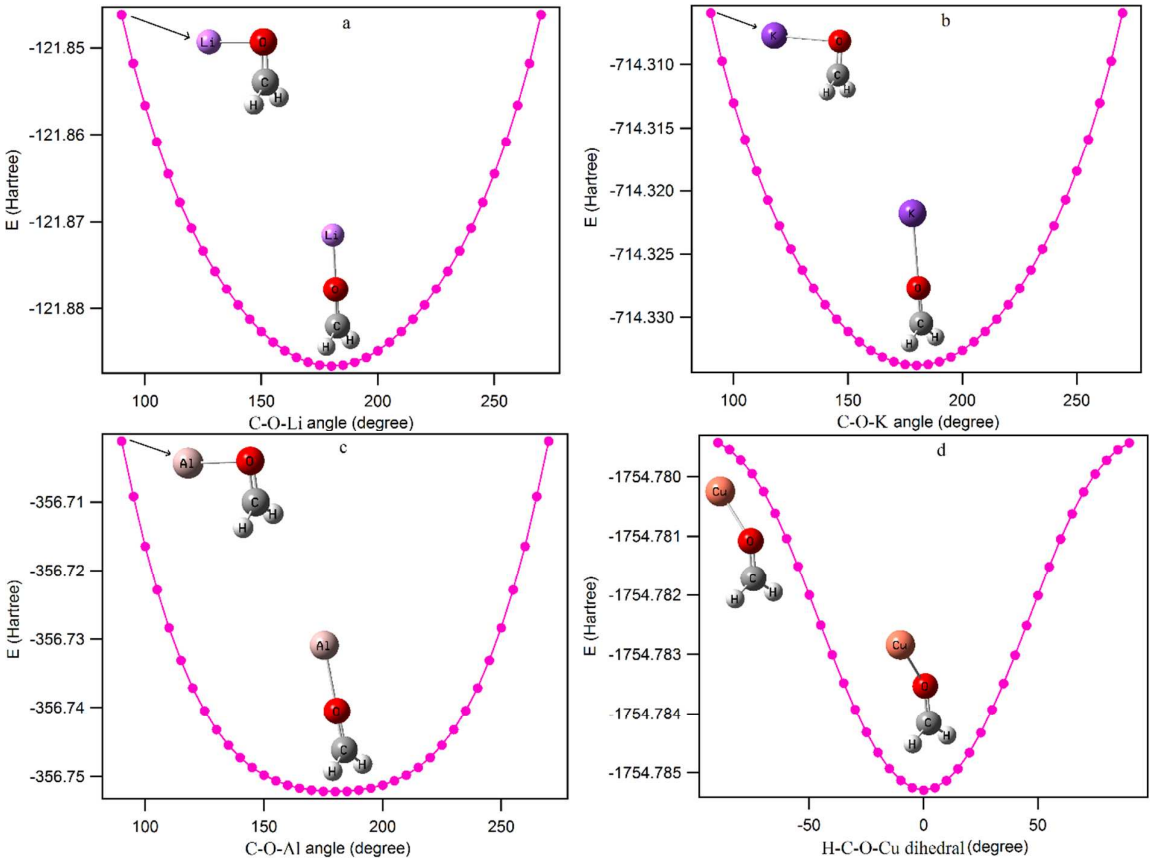

Figure S3. The potential energies obtained by scanning of the out of plane C=O-X angle in (a) CH_2O/Li^+, (b) CH_2O/K^+, (c) CH_2O/Al^+, and (d) CH_2O/Cu^+ adduct ions. In the case of CH_2O/Cu^+, the H-C-O-Cu dihedral was scanned. The results show that cations and CH_2O form planar adduct ions.

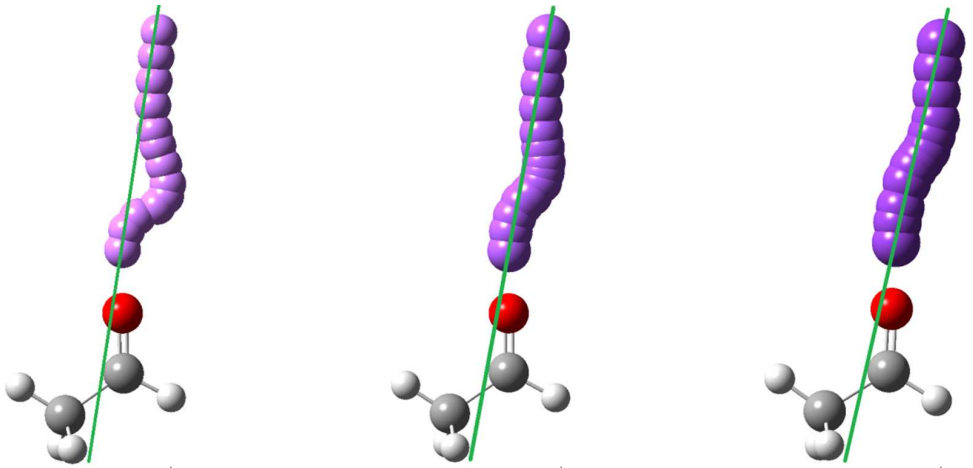

Figure S4. Geometry of the most stable structures of $[CH_3CHO/X]^+$ adduct ions obtained by scanning the C=O-X angles at different O-X bond, X= Li^+, Na^+ and K^+. The direction of the total dipole moment of acetaldehyde is indicated by a green line. At enough far distances, the ions are aligned with the direction of the dipole moment of acetaldehyde.

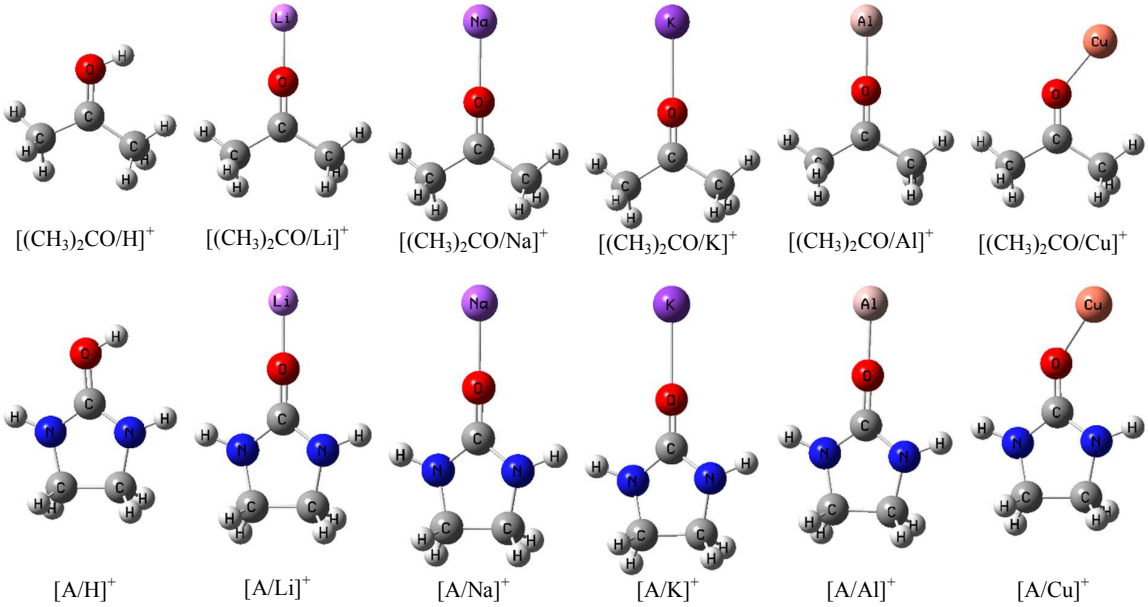

Figure S5. The optimized structures of adduct ions of acetone and imidazolin-2-one with H^+, Li^+, Na^+, K^+, Al^+, and Cu^+. A: imidazolin-2-one.

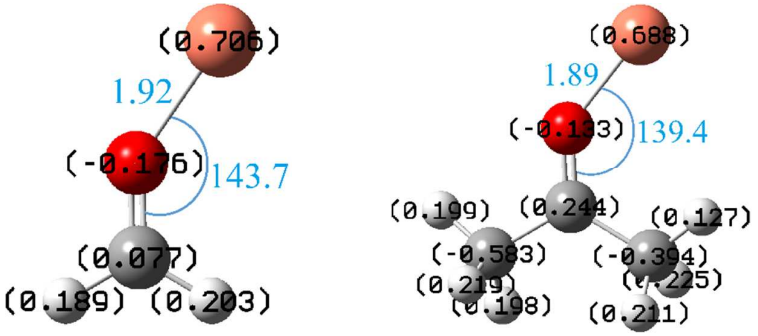

Figure S6. Comparison of charge distribution of $[(CH_3)_2CO/Cu]^+$ and $[CH_2O/Cu]^+$. Smaller charge on the Cu atom in $[(CH_3)_2CO/Cu]^+$ indicates more covalency of the $(CH_3)_2CO/Cu^+$ interaction. Although the effect of Cu/CH_3 repulsion in $[(CH_3)_2CO/Cu]^+$ is more than Cu/H repulsion in $[CH_2O/Cu]^+$, the C=O-Cu angle in $[(CH_3)_2CO/Cu]^+$ is smaller due to more covalency of the $(CH_3)_2CO/Cu^+$ interaction.

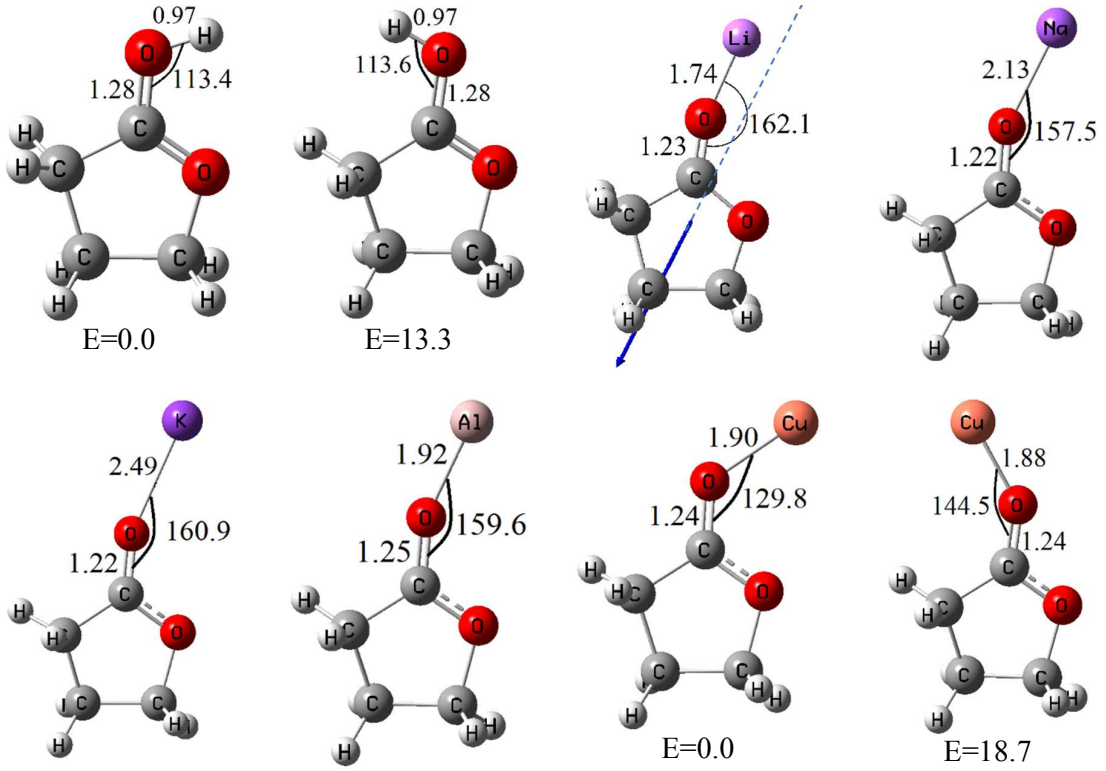

Figure S7. The optimized structures of γ-butyrolactone adduct ions of H^+, Li^+, Na^+, K^+, Al^+ and Cu^+. The energies, bond lengths and angles are in kJ/mol, angstrom (Å) and degree, respectively. The vector shows the direction of dipole moment of neutral γ-butyrolactone.

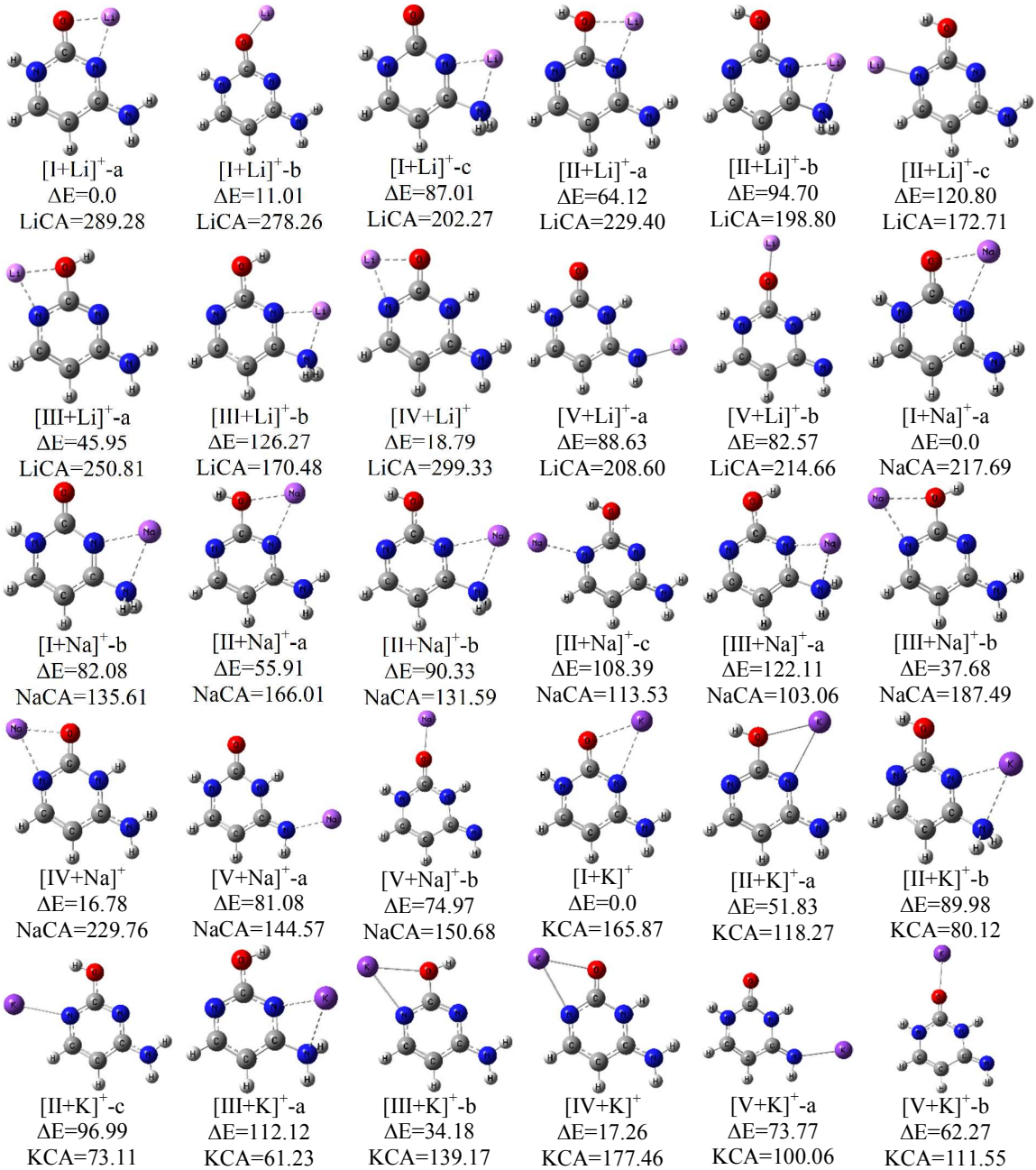

Figure S8. Structures of different isomers of alkali metal cation adducts of cytosine, optimized in gas phase at B3LYP/6-311++(d,p) level. The relative energies and cation affinities are in kJ/mol. The cation affinities are the enthalpies of reactions $[\text{Cytosine/X}]^+ \rightarrow \text{Cytosine} + X^+$ in gas phase. LiCA: Lithium cation affinity; NaCA: Sodium cation affinity; KCA: Potassium cation affinity.

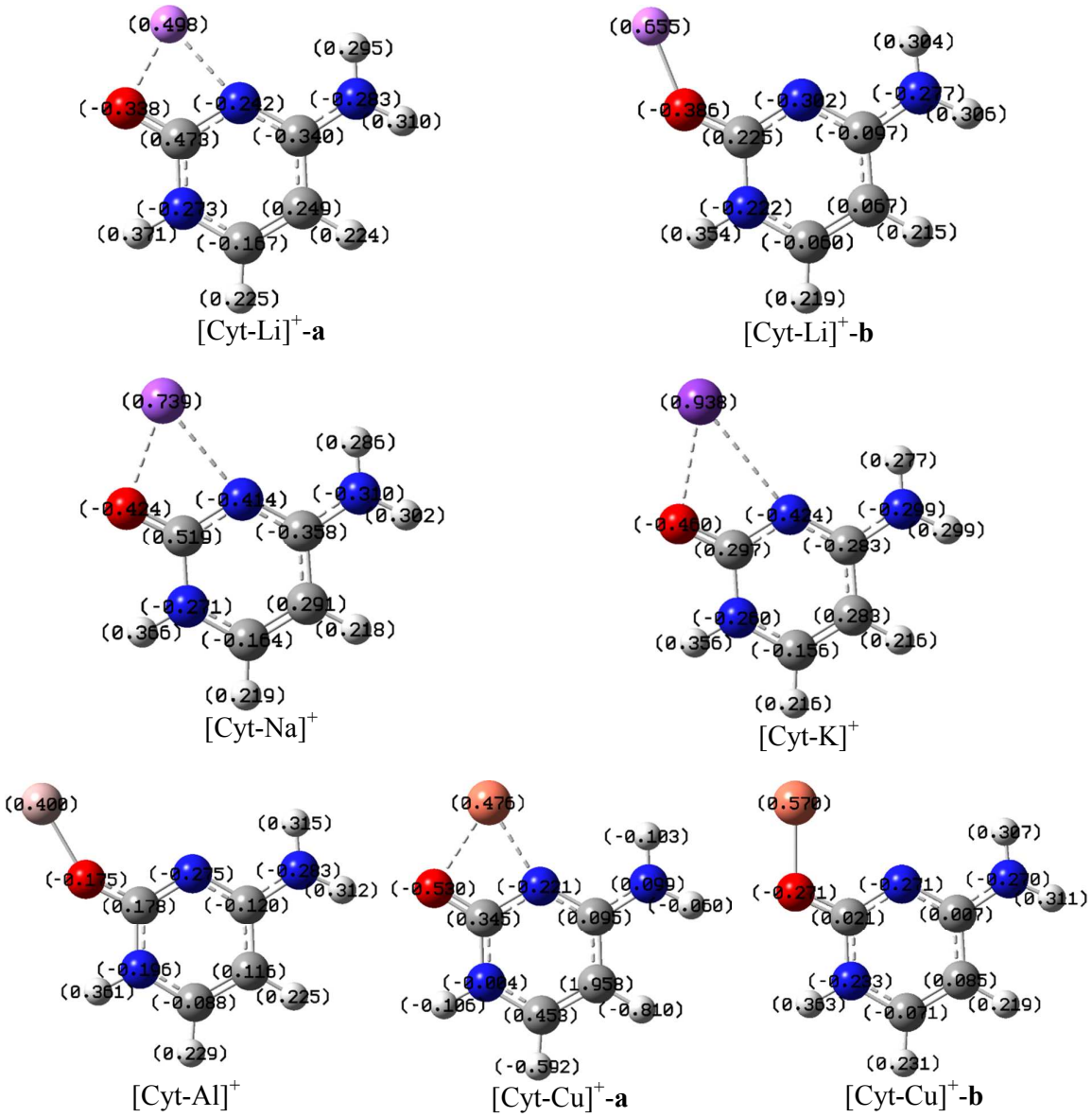

Figure S9. Mulliken charge distribution for the cytosine adduct computed by B3LYP/6-311++G(d,p) for all structures and B3LYP/aug-cc-PVDZ method for $[Cyt/Cu]^+$.

Cation	CH_2O	CH_2S	CH_2Se
H^+	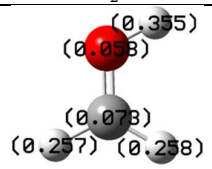	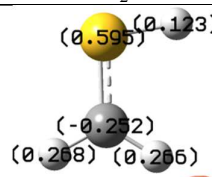	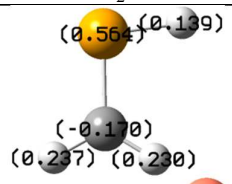
Cu^+	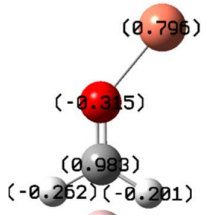	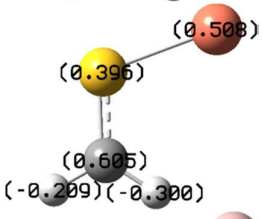	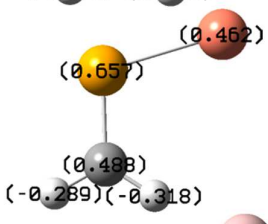
Al^+	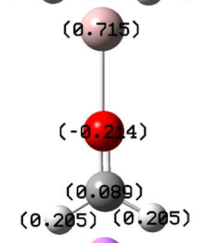	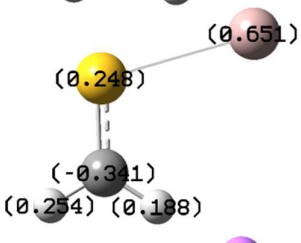	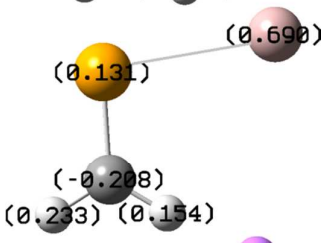
Li^+	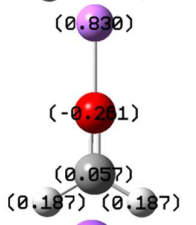	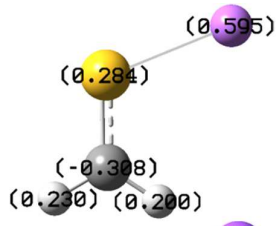	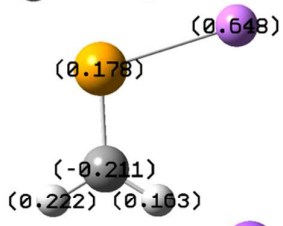
Na^+	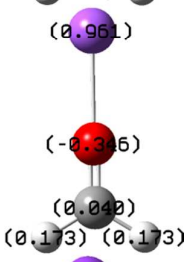	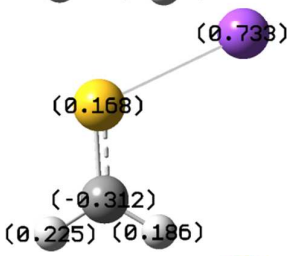	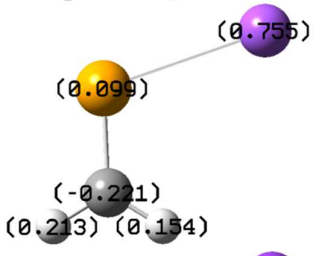
K^+	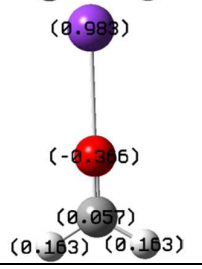	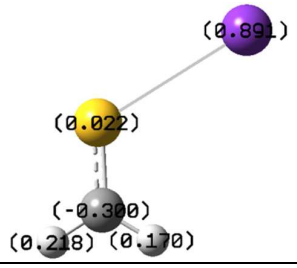	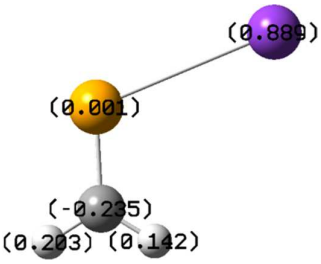

Figure S10. Mulliken charge distribution for the CH_2O, CH_2S and CH_2Se adduct ions computed by B3LYP/6-311++G(d,p) method. Only most stable structures are shown.